JACS
JOURNAL OF THE AMERICAN CHEMICAL SOCIETY

Communication

pubs.acs.org/JACS

Amplified Luminescence Quenching of Phosphorescent Metal–Organic Frameworks

Caleb A. Kent, Demin Liu, Thomas J. Meyer,* and Wenbin Lin*

Department of Chemistry, CB#3290, University of North Carolina, Chapel Hill, North Carolina 27599, United States

Supporting Information

ABSTRACT: Amplified luminescence quenching has been demonstrated in metal–organic frameworks (MOFs) composed of Ru(II)-bpy building blocks with long-lived, largely triplet metal-to-ligand charge-transfer excited states. Strong non-covalent interactions between the MOF surface and cationic quencher molecules coupled with rapid energy transfer through the MOF microcrystal facilitates amplified quenching with a 7000-fold enhancement of the Stern–Völmer quenching constant for methylene blue compared to a model complex.

Amplified luminescence quenching, a signal gain as a result of interactions between a sensing material and analytes accompanied by rapid energy migration, has been demonstrated in fluorescent conjugated polymers functionalized with receptor sites.[1] Dramatic emission quenching enhancements have been observed compared to monomeric models due to a "molecular wire" effect with the conjugated polymer facilitating energy migration over long distances. As the excited state migrates, it samples multiple receptor sites, thus requiring fewer receptor sites to be occupied by a quencher to elicit a significant spectroscopic response. Amplified fluorescence quenching of conjugated polymers is the basis of many practical sensing materials with extraordinarily high detection sensitivities.[2−4] To date, many types of conjugated polymers with singlet excited states have been shown to exhibit amplified quenching.[5−14] Phosphorescent materials capable of amplified quenching are potentially advantageous because the large red-shifts between light absorption and emission, as a result of intersystem crossing, can eliminate interference from the exciting light source in device configurations. Long-lived triplet excited states could allow excited-state migration over longer distances, and even higher levels of amplified quenching.

Attempts at developing amplified quenching with phosphorescent platinum(II)-acetylide polymers have been hindered by slow triplet diffusion.[15] Quenching enhancements of 75-fold have been demonstrated in conjugated polymers containing Ru-bpy complexes,[16] although excited-state migration is likely by site-to-site hopping rather than via the polymer backbone.[17]

Metal–organic frameworks (MOFs) represent a new class of structurally ordered and molecularly tunable hybrid materials.[18−33] In particular, our recent work demonstrated rapid energy migration over long distances[34] and efficient electron-transfer quenching at the interfaces of emitting MOFs.[35] We surmised that MOFs composed of Ru(II)-bpy building blocks offer a promising scaffold for amplified quenching based on their metal-to-ligand charge-transfer (MLCT) excited states. We report here a remarkable example of MOF-based amplified quenching by cationic quenchers with enhancements of up to 7000-fold compared to a model complex (Figure 1).

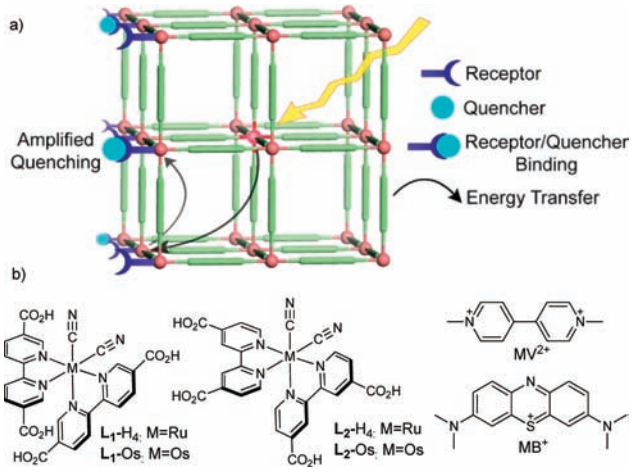

Figure 1. (a) Schematic diagram illustrating amplified quenching in MOFs and (b) chemical structures of the photoactive MOF building blocks and cationic quenchers (MV^{2+} and MB^{+}) used in this work. $\mathbf{L_1}$ and $\mathbf{L_2}$ refer to the building blocks for MOF **1** and **2**, respectively.

Crystals of $[Zn_5(\mathbf{L_1})_2\cdot(\mu\text{-}OH)\cdot(HCO_2)\cdot DMF\cdot 2H_2O]\cdot 6H_2O$ (**1**) were prepared by heating a mixture of $\mathbf{L_1}$-H_4 and $Zn(NO_3)_2$ in a mixture of DMF and H_2O for 2 weeks. Plate-like microcrystals of **1** of ∼200 nm in thickness and several micrometers in diameter were prepared by heating the above mixture and formic acid for 5 days. Microcrystals of **2** were synthesized as reported previously.[35]

1 adopts a three-dimensional framework structure that crystallizes in the monoclinic space group *P*2/*n*. In each asymmetric unit, there are two $\mathbf{L_1}$ ligands, five zinc atoms, four bridging cyano groups with the carbon atom coordinating to Ru and the nitrogen atom coordinating to Zn, two H_2O molecules and one DMF molecule coordinating to Zn centers, one bridging hydroxide group, and one chelating formate group. There are two crystallographically distinct four-metal-centered cores in which Ru and Zn are bridged by cyano groups (simplified as rectangles with different colors in Figure 2). They have a dihedral angle of 9.3° between the two planes formed by

Received: December 1, 2011
Published: February 13, 2012

   dx.doi.org/10.1021/ja211271m | *J. Am. Chem. Soc.* 2012, 134, 3991–3994

the two crystallographically different cores and a dihedral angle of 35.4° between the two crystallographically identical cores. **1** has open channels of 4.4 × 3.5 Å running along the *c* axis. PLATON[36] calculations indicated a void volume of 38.8%, which is consistent with the thermogravimetric analysis result (Supporting Information [SI]). The structure of **2** was described previously.[35]

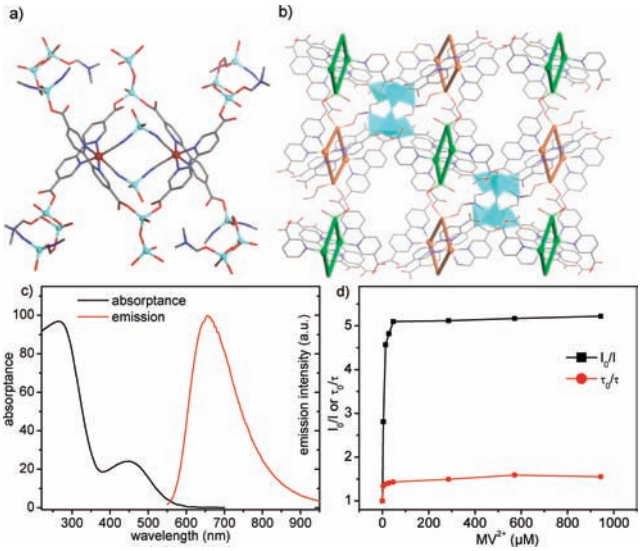

Figure 2. (a) Stick/ball model showing the four-Zn cores with cyano groups bridging between tetrahedral zinc and ruthenium centers in **1**. (b) Stick/polyhedral model showing the connection of the four-Zn cores to form the 3D framework structure of **1**. (c) Absorptance and emission spectra of **1**, and (d) steady-state and time-resolved SV plot of **1** with methyl viologen dication (MV^{2+}) in acetonitrile with 485 nm excitation (15 μM based on Ru). Emission decays were monitored at 670 nm. Absorptance values were calculated from transmission and diffuse reflectance measurements.

Excited-state quenching was investigated by both emission intensity and lifetime measurements on stirred suspensions of MOF microcrystals in degassed acetonitrile with added methyl viologen (MV^{2+}) or methylene blue (MB^+) as the quenchers. The MOF concentrations were 15 μM (based on Ru), as determined by the absorbance of the released building blocks after dissolution in 1 M HCl. Time-resolved emission from the MOFs was measured by using an Edinburgh FLSP920 spectrometer with sub-100 ps excitation pulses. Emission transients were satisfactorily fit to biexponential or triexponential decay functions for **1** and **2**, respectively, and are reported as average lifetimes (SI). Quenching results were analyzed by the Stern−Völmer (SV) expression in eq 1, in which I_0 is the integrated emission intensity without quencher and I is the intensity at a given quencher concentration. In a diffusional system, the SV constant, K_{SV}, is given by eq 2, with k_q being the quenching rate constant and τ_0 being the excited-state lifetime without added quencher. When static quenching is the dominant mechanism, K_{SV} is given by eq 3, with K being the surface interaction constant and N_S being the number of surface sites sampled by the excited state.

$$I_0/I = 1 + K_{SV}[Q] \quad (1)$$

$$K_{SV(diffusional)} = k_q\tau_0 \quad (2)$$

$$K_{SV(static)} = KN_s \quad (3)$$

1 emits at λ_{max} = 655 nm with a lifetime of 150 ns. Emission quenching of **1*** by MV^{2+} is efficient at low quencher concentrations. From the linear region of plots of I_0/I vs $[MV^{2+}]$, $K_{SV} = 4.2 \times 10^5$ M^{-1} for **1** with half-quenching reached at $[MV^{2+}] = 2.4$ μM. Given the SV relationship in eq 2, the apparent quenching rate constant is $k_{q,app} = 2.8 \times 10^{12}$ M^{-1} s^{-1}. This value is more than 2 orders of magnitude higher than the diffusion-controlled limit under these conditions, ruling out diffusional quenching. The MOF surface is partially terminated with carboxylate groups, promoting static quenching by binding MV^{2+} via ionic interactions on the surface (see below).

Emission quenching saturates at $[MV^{2+}] \approx 50$ μM, with 20% of the original emission intensity unquenched at $I_0/I \approx 5$ (Figure 2d). A microscopic model consistent with the experimental observations is shown in Scheme 1. In this model, initial surface binding of the cation occurs by an ionic interaction with the surface carboxylates (K in eq 4). The steady-state SV plot increases linearly with added MV^{2+} up to 5 μM. Quenching occurs by intra-MOF energy transfer via site-to-site hopping to the interface (k_{EN} in eq 6), where electron-transfer quenching of a surface excited state occurs (k_{ET} in eq 7).[37] Electron-transfer quenching is in competition with excited-state decay ($1/\tau_o$ in eq 8). For **1**, quenching is incomplete even at high quencher concentrations because of competitive excited-state decay. Approximately 20% of the excited states remain unquenched even though quenching is expected to be complete at the surface.

Scheme 1. MOF Surface Quenching by MV^{2+} [a]

$$(Ru_c^{II})(Ru_s^{II}\text{-bpy-COO}^-) + MV^{2+} \rightarrow (Ru_c^{II})(Ru_s^{II}\text{-bpy-COO}^-,MV^{2+}) \quad (K) \quad (4)$$

$$(Ru_c^{II})(Ru_s^{II}\text{-bpy-COO}^-,MV^{2+}) + h\nu \rightarrow (Ru_c^{II}*)(Ru_s^{II}\text{-bpy-COO}^-,MV^{2+}) \quad (5)$$

$$(Ru_c^{II}*)(Ru_s^{II}\text{-bpy-COO}^-,MV^{2+}) \rightarrow (Ru_c^{II})(Ru_s^{II*}\text{-bpy-COO}^-,MV^{2+}) \quad (k_{EN}) \quad (6)$$

$$(Ru_c^{II})(Ru_s^{II*}\text{-bpy-COO}^-,MV^{2+}) \rightarrow (Ru_c^{II})(Ru_s^{III}\text{-bpy-COO}^-,MV^{+}) \quad (k_{ET}) \quad (7)$$

$$(Ru_c^{II}*)(Ru_s^{II}\text{-bpy-COO}^-,MV^{2+}) \rightarrow (Ru_c^{II})(Ru_s^{II}\text{-bpy-COO}^-,MV^{2+}) + h\nu \quad (1/\tau_o) \quad (8)$$

[a] Ru_c and Ru_s are core and surface sites.

2 emits with λ_{max} = 630 nm and τ = 900 ns and is also partially terminated with carboxylate groups which can participate in surface ionic interactions. At low MV^{2+} concentrations $K_{SV} = 3.2 \times 10^6$ M^{-1} at [**2**] = 15 μM (based on total Ru). This results in a $k_{q,app} = 3.6 \times 10^{12}$ M^{-1} s^{-1} which, again, is well beyond the diffusion-controlled limit and consistent with static quenching as illustrated in Scheme 1. Based on lifetime measurements on Os^{II}-doped MOFs (SI), intra-MOF energy transfer in **2** is more rapid than in **1**, and quenching of **2*** proceeds essentially to completion as the concentration of MV^{2+} is increased. Quenching was 97% complete at $[MV^{2+}] = 2.8$ μM, with only 0.31 μM of MV^{2+} required for half-quenching. This is several orders of magnitude less than required for half-quenching of **2*** by the neutral quenchers 1,4-benzoquinone (7400 μM) and *N*,*N*,*N*′,*N*′-tetramethylbenzidine (760 μM).[35]

The magnitude of K_{SV} is also dependent on the MOF concentration, with K_{SV} increasing as the MOF concentration decreases. This is a predicted result of the model in Scheme 1. It arises from a competition for MV^{2+} by a limited number of

surface sites. At lower MOF concentrations, there is a higher concentration of quenchers available per MOF particle.

The steady-state emission SV plot in Figure 3a displays upward curvature or "superlinear" behavior. We reported

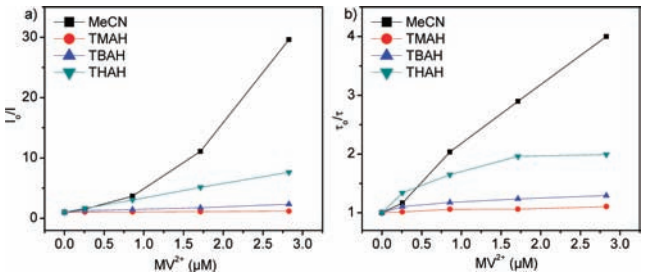

Figure 3. (a) Steady-state (I/I_0) and (b) time-resolved (τ/τ_0) SV plots of **2** (15 μM based on Ru) with methyl viologen (MV^{2+}) in acetonitrile with 0.1 M tetra-*N*-alkylammonium hexafluorophosphate electrolytes (TMAH, TBAH, and THAH are the methyl, *n*-butyl, and *n*-hexyl derivatives) at 485 nm excitation. Emission decay was monitored at 630 nm.

similar behavior with neutral quenchers with small association constants arising from simultaneous static and dynamic quenching.[35] Given the absence of diffusional quenching for MV^{2+}, there must be a different origin for the present systems. Upward curvature is a common observation for polymer-based amplified quenching,[6,8] where it has been explained by invoking a "sphere of action" quenching mechanism[38] or as a result of aggregation of polymer fluorophores.[6] Superlinear behavior in the MOFs may arise from aggregation induced by neutralization of the negatively charged MOF surface by cationic quenchers. When samples are left unstirred, a suspension with added quencher settles faster than without quencher.

Emission quenching efficiencies for **2*** by MV^{2+} were investigated with added 0.1 M tetra-*N*-alkylammonium salts, $(NR_4)PF_6$. Steady-state SV plots (Figure 3a) were no longer superlinear. The magnitude of K_{SV} with added electrolyte increased with cation size in the order NMe_4^+ ($K_{SV} = 6.2 \times 10^4$ M^{-1}) < N(*n*-butyl)$_4^+$ ($K_{SV} = 4.4 \times 10^5$ M^{-1}) < N(*n*-hexyl)$_4^+$ ($K_{SV} = 2.4 \times 10^6$ M^{-1}). This dependence is qualitatively consistent with stronger electrostatic interactions with surface carboxylate sites as the cation radius decreases, presumably enhancing the surface ion-exchange equilibrium, $-COO^-,NR_4^+ + MV^{2+} \leftrightarrow -COO^-,MV^{2+} + NR_4^+$.

Amplified quenching of **2*** by methylene blue cation (MB^+) was also observed (Figure 4). At [Ru] = 15 μM, $K_{SV} = 8.9 \times 10^6$ M^{-1}. At [Ru] = 3 μM, K_{SV} increased to 2.7×10^7 M^{-1}. Emission interferences occur for the quenching of **2*** with MB^+, which are minimized by integrating the emission intensity from 750 to 850 nm (SI). With MB^+, the MOF−quencher interaction can be easily observed by the eye. Mixing of a MOF suspension and a methylene blue solution followed by centrifugation results in noticeable color loss in the supernatant and a change in color of the MOF microcrystals from bright orange-red to green.

A surface interaction constant for MB^+ and **2** (15 μM) was estimated by calculating the amount of surface-adsorbed dye based on absorbance changes in the supernatant. Data acquired over the range of 1−3 μM MB^+, fitted to a Langmuir model, gave $K = 7.5 \times 10^4$ M^{-1} (SI). With this value and the interpretation of K_{SV} for static quenching in eq 3, the excited state is estimated to sample ~120 surface sites during its

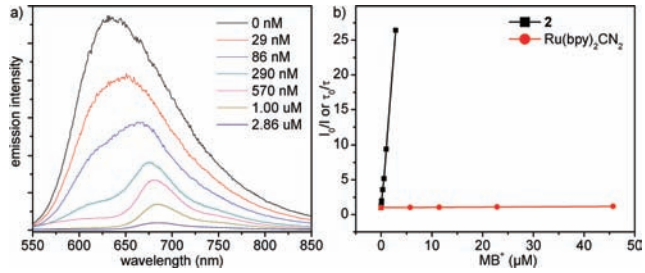

Figure 4. (a) Steady-state emission of **2** (15 μM based on Ru) in acetonitrile with added methylene blue (MB^+) upon 420 nm excitation and (b) SV analysis of **2** with added MB^+ by steady-state emission measurements and of $Ru(bpy)_2CN_2$ by time-resolved emission measurements. The emission intensity was integrated between 750 and 850 nm to minimize complications from absorption and emission from methylene blue. The first 50 ns after excitation was not included in the lifetime decay fits to avoid the contribution from methylene blue fluorescence at λ_{max} = 676 nm.

lifetime. At [MB^+] > 3 μM, the data deviate from Langmuir behavior, apparently due to MB^+---MB^+ aggregation on the MOF surface. The onset of aggregation is evident by the appearance of emission at 570 nm (SI), consistent with previous reports of ground-state MB^+ aggregation leading to blue shifts in absorption and emission spectra.[39]

Even though the interaction of **2** with both MV^{2+} and MB^+ is irreversible, the powder X-ray diffraction pattern of **2** is unchanged after exposure to MB^+, consistent with a surface interaction without structural disruption by intercalation throughout the MOF framework (SI).

Quenching of **2*** by MB^+, as with MV^{2+}, probably occurs by oxidative electron transfer. Quenching of the Os analogue of **2** (**2**-Os) by MB^+ (Figure 5) is also rapid and does occur by

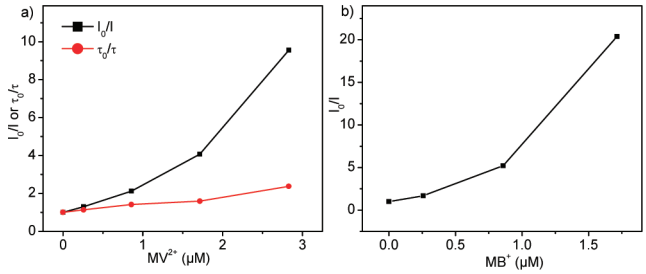

Figure 5. (a) Steady-state and time-resolved SV plots for **2**-Os (15 μM based on Os) in acetonitrile with added MV^{2+} upon 485 nm excitation. The decay was monitored at 740 nm. (b) Steady-state SV plot of **2**-Os with added MB^+ in acetonitrile upon 420 nm excitation. The emission intensity was integrated from 850 to 950 nm to minimize complications from emission of methylene blue (SI).

electron transfer. Energy transfer is unfavorable in this case since the thermally equilibrated excited state is too low in energy to undergo energy transfer to MB^+ (SI). The driving forces for electron-transfer quenching for **2*** and **2***-Os should be comparable. Excited-state oxidation potentials for Ru(bpy)$_3^{2+*}$ and Os(bpy)$_3^{2+*}$ only differ by ~0.1 V.[40]

2*-Os is quenched by both MV^{2+} and MB^+ in acetonitrile with $K_{SV} = 1.3 \times 10^6$ and 5.1×10^6 M^{-1}, respectively. Upward curvature is also observed in the SV plots. The magnitudes of the SV constants in this case are half those for **2***, even though the emission lifetime decreases from 900 ns for **2*** to 30 ns for **2**-Os*. This observation points to a considerably enhanced rate

dx.doi.org/10.1021/ja211271m | *J. Am. Chem. Soc.* 2012, 134, 3991−3994

of intra-MOF energy transfer for **2**-Os*, k_{EN} in eq 6, and a possible role for long-range singlet−singlet Förster transfer. Spin−orbit coupling is larger for Os with MLCT states ∼30% singlet in character, promoting long-range dipole−dipole Förster transfer.[41] The relative rates for Ru^{II}*→Ru^{II} compared to Os^{II}*→Os^{II} energy transfer can be estimated based on the assumption that the K_{SV} is proportional to the number of energy-transfer steps by the excited state. This analysis shows that Os^{II}*→Os^{II} transfer is 12−17 times more rapid than Ru^{II}*→Ru^{II} transfer (SI).

Quenching studies were also conducted on $Ru(bpy)_2CN_2$ with MB^+ in order to estimate the degree of amplification of emission quenching in the MOF compared to the neutral model compound in solution (Figure 4b). In order to accurately quantify the quenching efficiency in solution, K_{SV} was calculated from time-resolved data, with the first 50 ns of data excluded to avoid MB^+ emission. The quenching of $Ru(bpy)_2CN_2$ by MB^+ in solution is far less efficient, with $K_{SV} = 3.9 \times 10^3\ M^{-1}$. Comparison with **2** gives an amplification factor of 7000, which is 2 orders of magnitude higher than those observed in earlier studies based on conjugated polymers with covalently linked Ru-bpy complexes.[16] This work thus demonstrates the remarkable ability of phosphorescent MOFs in amplifying luminescence quenching as a result of long-distance intra-MOF energy transfer and efficient electron-transfer quenching at the interface. The tunability and crystalline structures of MOFs should allow for the design of systems for selective sensing of chosen analytes and merits further investigation.

■ ASSOCIATED CONTENT

Ⓢ Supporting Information

Experimental procedures and characterization data. This material is available free of charge via the Internet at http://pubs.acs.org.

■ AUTHOR INFORMATION

Corresponding Author

wlin@unc.edu; tjmeyer@unc.edu

Notes

The authors declare no competing financial interest.

■ ACKNOWLEDGMENTS

This material is based upon work supported as part of the UNC EFRC: Center for Solar Fuels, an Energy Frontier Research Center funded by the U.S. Department of Energy, Office of Science, Office of Basic Energy Sciences, under Award No. DE-SC0001011 (for supporting C.A.K.). D.L. was supported by a NSF grant to W.L. (DMR-0906662).

■ REFERENCES

(1) Zhou, Q.; Swager, T. M. *J. Am. Chem. Soc.* **1995**, *117*, 12593.
(2) Yang, J. S.; Swager, T. M. *J. Am. Chem. Soc.* **1998**, *120*, 5321.
(3) Yang, J. S.; Swager, T. M. *J. Am. Chem. Soc.* **1998**, *120*, 11864.
(4) Narayanan, A.; Varnavski, O. P.; Swager, T. M.; Goodson, T. III *J. Phys. Chem. C* **2008**, *112*, 881.
(5) McQuade, D. T.; Pullen, A. E.; Swager, T. M. *Chem. Rev.* **2000**, *100*, 2537.
(6) Thomas, S. W. III; Joly, G. D.; Swager, T. M. *Chem. Rev.* **2007**, *107*, 1339.
(7) Liu, Y.; Ogawa, K.; Schanze, K. S. *J. Photochem. Photobiol. C−Photochem. Rev.* **2009**, *10*, 173.
(8) Chen, L. H.; McBranch, D. W.; Wang, H. L.; Helgeson, R.; Wudl, F.; Whitten, D. G. *Proc. Natl. Acad. Sci. U.S.A.* **1999**, *96*, 12287.
(9) Tan, C. Y.; Pinto, M. R.; Schanze, K. S. *Chem. Commun.* **2002**, 446.
(10) Fan, C. H.; Plaxco, K. W.; Heeger, A. J. *J. Am. Chem. Soc.* **2002**, *124*, 5642.
(11) Fan, C. H.; Wang, S.; Hong, J. W.; Bazan, G. C.; Plaxco, K. W.; Heeger, A. J. *Proc. Natl. Acad. Sci. U.S.A.* **2003**, *100*, 6297.
(12) Achyuthan, K. E.; Bergstedt, T. S.; Chen, L.; Jones, R. M.; Kumaraswamy, S.; Kushon, S. A.; Ley, K. D.; Lu, L.; McBranch, D.; Mukundan, H.; Rininsland, F.; Shi, X.; Xia, W.; Whitten, D. G. *J. Mater. Chem.* **2005**, *15*, 2648.
(13) Jones, R. M.; Lu, L. D.; Helgeson, R.; Bergstedt, T. S.; McBranch, D. W.; Whitten, D. G. *Proc. Natl. Acad. Sci. U.S.A.* **2001**, *98*, 14769.
(14) Tan, C. Y.; Alas, E.; Muller, J. G.; Pinto, M. R.; Kleiman, V. D.; Schanze, K. S. *J. Am. Chem. Soc.* **2004**, *126*, 13685.
(15) Haskins-Glusac, K.; Pinto, M. R.; Tan, C. Y.; Schanze, K. S. *J. Am. Chem. Soc.* **2004**, *126*, 14964.
(16) Liu, Y.; Jiang, S. J.; Schanze, K. S. *Chem. Commun.* **2003**, 650.
(17) Fleming, C. N.; Maxwell, K. A.; DeSimone, J. M.; Meyer, T. J.; Papanikolas, J. M. *J. Am. Chem. Soc.* **2001**, *123*, 10336.
(18) Seo, J. S.; Whang, D.; Lee, H.; Jun, S. I.; Oh, J.; Jeon, Y. J.; Kim, K. *Nature* **2000**, *404*, 982.
(19) Evans, O. R.; Lin, W. *Acc. Chem. Res.* **2002**, *35*, 511.
(20) Kitagawa, S.; Kitaura, R.; Noro, S.-I. *Angew. Chem., Int. Ed.* **2004**, *43*, 2334.
(21) Kaye, S. S.; Dailly, A.; Yaghi, O. M.; Long, J. R. *J. Am. Chem. Soc.* **2007**, *129*, 14176.
(22) Farha, O. K.; Hupp, J. T. *Acc. Chem. Res.* **2010**, *43*, 1166.
(23) Chen, B.; Wang, L.; Xiao, Y.; Fronczek, F. R.; Xue, M.; Cui, Y.; Qian, G. *Angew. Chem., Int. Ed.* **2009**, *48*, 500.
(24) Furukawa, H.; Ko, N.; Go, Y.-B.; Aratani, N.; Choi, S. B.; Choi, E.; Yazaydin, A. O.; Snurr, R. Q.; O'Keeffe, M.; Kim, J.; Yaghi, O. M. *Science* **2010**, *329*, 424.
(25) Rieter, W. J.; Taylor, K. M. L.; An, H.; Lin, W.; Lin, W. *J. Am. Chem. Soc.* **2006**, *128*, 9024.
(26) Rieter, W. J.; Pott, K. M.; Taylor, K. M. L.; Lin, W. *J. Am. Chem. Soc.* **2008**, *130*, 11584.
(27) Ma, L.; Falkowski, J. M.; Abney, C.; Lin, W. *Nat. Chem.* **2010**, *2*, 838.
(28) Lan, A.; Li, K.; Wu, H.; Olsson, D. H.; Emge, T. J.; Ki, W.; Hong, M.; Li, J. *Angew. Chem., Int. Ed.* **2009**, *48*, 2334.
(29) Li, J.-R.; Kuppler, H.-C.; Zhou, H.-C. *Chem. Soc. Rev.* **2009**, *38*, 1477.
(30) Wu, C.-D.; Hu, A.; Zhang, L.; Lin, W. *J. Am. Chem. Soc.* **2005**, *127*, 8940.
(31) Xie, Z.; Ma, L.; deKrafft, K. E.; Jin, A.; Lin, W. *J. Am. Chem. Soc.* **2009**, *132*, 922.
(32) D'Alessandro, D. M.; Smit, B.; Long, J. R. *Angew. Chem., Int. Ed.* **2010**, *49*, 6058.
(33) Shustova, N. B.; McCarthy, B. D.; Dinca, M. *J. Am. Chem. Soc.* **2011**, *133*, 20126.
(34) Kent, C. A.; Mehl, B. P.; Ma, L. Q.; Papanikolas, J. M.; Meyer, T. J.; Lin, W. B. *J. Am. Chem. Soc.* **2010**, *132*, 12767.
(35) Kent, C. A.; Liu, D.; Ma, L.; Papanikolas, J. M.; Meyer, T. J.; Lin, W. *J. Am. Chem. Soc.* **2011**, *133*, 12940.
(36) Spek, A. L. *J. Appl. Crystallogr.* **2003**, *36*, 7.
(37) Bock, C. R.; Meyer, T. J.; Whitten, D. G. *J. Am. Chem. Soc.* **1974**, *96*, 4710.
(38) Wang, J.; Wang, D. L.; Miller, E. K.; Moses, D.; Bazan, G. C.; Heeger, A. J. *Macromolecules* **2000**, *33*, 5153.
(39) Severino, D.; Junqueira, H. C.; Gugliotti, M.; Gabrielli, D. S.; Baptista, M. S. *Photochem. Photobiol.* **2003**, *77*, 459.
(40) Hoselton, M. A.; Lin, C. T.; Schwarz, H. A.; Sutin, N. *J. Am. Chem. Soc.* **1978**, *100*, 2383.
(41) von Arx, M. E.; Burattini, E.; Hauser, A.; van Pieterson, L.; Pellaux, R.; Decurtins, S. *J. Phys. Chem. A* **2000**, *104*, 883.